Water and Backbone Dynamics in a Hydrated Protein

Galina Diakova,[†] Yanina A. Goddard,[†] Jean-Pierre Korb,[‡] and Robert G. Bryant[†*]
[†]Chemistry Department, University of Virginia, Charlottesville, Virginia; and [‡]Physique de la Matière Condensée, Ecole Polytechnique, CNRS, Palaiseau, France

ABSTRACT Rotational immobilization of proteins permits characterization of the internal peptide and water molecule dynamics by magnetic relaxation dispersion spectroscopy. Using different experimental approaches, we have extended measurements of the magnetic field dependence of the proton-spin-lattice-relaxation rate by one decade from 0.01 to 300 MHz for ^{1}H and showed that the underlying dynamics driving the protein ^{1}H spin-lattice relaxation is preserved over 4.5 decades in frequency. This extension is critical to understanding the role of ^1H_2O in the total proton-spin-relaxation process. The fact that the protein-proton-relaxation-dispersion profile is a power law in frequency with constant coefficient and exponent over nearly 5 decades indicates that the characteristics of the native protein structural fluctuations that cause proton nuclear spin-lattice relaxation are remarkably constant over this wide frequency and length-scale interval. Comparison of protein-proton-spin-lattice-relaxation rate constants in protein gels equilibrated with ^2H_2O rather than ^1H_2O shows that water protons make an important contribution to the total spin-lattice relaxation in the middle of this frequency range for hydrated proteins because of water molecule dynamics in the time range of tens of ns. This water contribution is with the motion of relatively rare, long-lived, and perhaps buried water molecules constrained by the confinement. The presence of water molecule reorientational dynamics in the tens of ns range that are sufficient to affect the spin-lattice relaxation driven by ^{1}H dipole-dipole fluctuations should make the local dielectric properties in the protein frequency dependent in a regime relevant to catalytically important kinetic barriers to conformational rearrangements.

INTRODUCTION

Water molecule dynamics in and around proteins may contribute to the molecular motions that are critical to catalytic and biological function. The water-proton-spin-lattice-relaxation-rate constant, $1/T_1$, is dependent on water dynamics and is a primary determinant of contrast in magnetic images. For tissues as well as isolated immobilized protein systems, the spin-lattice-relaxation-rate constant for the water protons is a function of magnetic field strength and described by a power law in the proton Larmor frequency (1–7). This magnetic field dependence derives from the dynamics of protein-bound water and magnetic coupling of the water protons to the protons of nonrotating macromolecular components of the tissue, particularly proteins (8). This intermolecular magnetic coupling transfers the magnetic field dependence of the immobilized protein protons to the bulk water protons. Depending on composition, the effects of finite magnetization-transfer rates may limit the water-proton-relaxation-rate constant at the lowest magnetic field strengths and cause a low field plateau for this contribution. Although spectral resolution for a rotationally immobilized protein is low, the dynamic information available is not limited by the protein rotational correlation time. Therefore, it is possible to study protein and water dynamics at low frequencies.

The immobilized protein is magnetically a solid in the sense that the dipole-dipole couplings among the protons are not averaged by rapid rotational motion; the resulting proton NMR line width is large, on the order of 35 kHz. The critical consequence of this unaveraged dipolar coupling is that spin-spin communication among the protein protons is rapid (9).

In the nonrotating protein, these strong dipolar couplings bring the protons into equilibrium with each other rapidly with time constants on the order of the transverse relaxation time, which is ~10 μs (10). Thus, motion causing ^{1}H spin-lattice relaxation anywhere in the protein causes relaxation in the whole strongly coupled protein-spin system. In this study, we focus on the dynamics in a pure protein system although there are important consequences for more complex systems such as tissues.

The underlying nuclear spin-lattice-relaxation mechanism for protein protons derives from structural fluctuations that modulate interproton dipolar couplings (4,11). A ''spin-fracton'' theory for a direct spin-lattice-relaxation process has accounted successfully for the frequency and temperature dependence of ^{1}H spin-lattice relaxation in immobilized protein systems (3,6,12). The temperature dependence for the protein-proton relaxation is unusual in that the rate constant is a linear function of temperature in the low field regime as predicted by this theory and confirmed experimentally over a temperature range of 150 K (13). The term ''fracton'' is appropriate because the system is not periodic and the excitations are localized on a length scale determined by the structural elements of the protein. The basic idea is that the proton relaxation derives from small changes in the relative positions and orientations of protons that are caused by structural fluctuations. The spin-fracton theory uses a vibrational model for the direct spin-phonon process, as

Submitted July 23, 2009, and accepted for publication September 28, 2009.

*Correspondence: rgb4g@virginia.edu

Editor: Josh Wand.

0006-3495/10/01/0138/9 $2.00

doi: 10.1016/j.bpj.2009.09.054

opposed to a Raman process. Unlike a three-dimensional (3D) ionic solid, the dynamical connectivity within a protein is not uniform in three-space because the polypeptide folds with side-chains of differing volume and packing characteristics. The nonuniform connectivity reduces the number of propagation pathways the model for the vibrational density of states has a different frequency dependence than that associated with the 3D model of Debye (14). The Gaussian network models for protein dynamics use the same class of ideas to construct a network based on the proximity between structural units in the folded structure; the dynamical connectivity is reduced and the vibrational density of states deduced from this approach is characterized by the spectra dimension d_s that is substantially <3. Thus, $d_s - 1$ is much less than the Debye value of $d - 1$ where $d = 3$ for a uniformly connected 3D solid (15,16). This spectral dimension enters the spin-fracton theory through the vibrational density of states that determines, in part, the magnetic field dependence of the relaxation-rate constant. In the same spirit, the theory also includes the dimensionality d_f for the distribution of mass in space, which is fractal and close to, but not precisely, 3 (17,18). A final aspect of the spin-fracton model is the nature of the spatial localization of the structural disturbances. The spatial extent, ℓ_α, ranges from a minimal size on the order of the monomer unit to the length of the polypeptide, and the spatial extent is related to the frequency of the fluctuation ω_α. For a region of size, ℓ_α, modes for which $\omega > \omega_\alpha$ are strongly overdamped. Scaling arguments show that the product $\ell_\alpha^{d_f}\omega_\alpha^{d_s}$ is a constant, thus, there is an anomalous dispersion relation $q_\alpha = 1/\ell_\alpha \propto \omega_\alpha^{d_s/d_f}$ between q-space and frequency, instead of the usual dispersion relation $q \propto 1/\omega$ encountered in crystals. We note that these ideas are not new, nor are they unique to models for spin-lattice relaxation; the same parameters enter recent theoretical studies of proteins (16).

Halle and co-workers have criticized this approach and built a model (EMOR) for the magnetic field dependence of spin-lattice relaxation that depends on the dynamics of the water-molecule exchange rates as the source of the critical fluctuations in hydrated protein systems (19–21). The essence of the idea applied to ^{1}H relaxation is that the dipolar couplings are interrupted by water molecule or ^{1}H exchange processes that lead to a dispersion like that seen for pure water at very low frequencies because of exchange interruption of the rotationally invariant ^{1}H-^{17}O scalar coupling. An individual water binding site then contributes a Lorentzian dispersion, but the power-law shape is achieved by a broad distribution of exchange times. A critical explicit assumption for this model is that the cross-relaxation among the protein protons is negligible. As a result, the water spins sense only adjacent protein spins, not the whole protein-proton-spin population or its magnetic field dependence. In this case, the effective dynamics are only those that modulate the intramolecular water dipolar coupling or the water-proton coupling to nearest neighbor protein protons. This assumption effectively suppresses the coupling of the magnetic field dependence of the protein-proton population with the water-proton-field dependence. The water molecule exchange processes should be thermally activated so that an exponential dependence on temperature is expected; however, the apparent temperature dependence may be affected by the different activation energies associated with the distribution of exchange sites. These authors suggest that the dipolar coupling between the water and the protein is quenched by the exchange process, and therefore, unimportant. Although first order dipolar splittings of ^1H_2O are rarely observed and the mixing caused by chemical exchange would suppress them, the spin relaxation depends on the perturbation carried to second order, and the coupling is not attenuated by the exchange although the coupling time may be reduced. Thus, the chemical exchange need not make the intermolecular cross-relaxation negligible. The importance of exchange modulation and cross-relaxation depends on the efficiency of the relaxation coupling that is dependent on several factors including composition, frequency, and temperature.

We note that although there are good reasons to use the spin-fracton model in this analysis, the conclusions concerning local water molecule dynamics do not depend on it. One could equivalently proceed with a strictly numerical parameterization of the background protein-proton-spin-lattice-relaxation rates where $1/T_{1\text{protein}} = A\omega^{-b}$.

Previous studies of proton-spin-lattice relaxation as a function of water content in protein systems indicated that the apparent power-law exponent was a function of the water content (5). Such a dependence is not unreasonable because resolution is generally lost with dehydration in scattering experiments and it is likely that the protein structure responds to increased electrostatic strain caused by removal of water electric dipoles and hydrogen bonds (22,23). Nevertheless, we show here that the power-law exponent describing the field dependence of ^{1}H spin-lattice relaxation does not change with hydration over nearly 5 decades in Larmor frequency when a sufficiently wide range of frequencies is studied. Using deuterium for proton isotope substitution, we show that hydration of lyophilized protein with deuterated water even up to the level of 100 g water/15 g protein in a cross-linked gel, leaves the magnetic field dependence of the proton-spin-lattice relaxation unperturbed with a power law, $1/T_1 = A\omega^{-b}$, and $b = 0.78 \pm 0.06$. However, when the water molecules bear protons, the local motion of the water protons in long-lived protein sites provides another spin-relaxation contribution in the range of several MHz that may be resolved from the protein backbone dynamics and distort the appearance of the underlying magnetic field dependence. For bovine serum albumin (BSA), this contribution from rare bound-water molecule motion has an effective correlation time of tens of ns.

MATERIALS AND METHODS

BSA (Fraction V, Sigma-Aldrich, St. Louis, MO) was dialyzed against deionized water and lyophilized to constant weight using a mechanical vacuum

at room temperature. To make BSA/H_2O gels 0.1 mL of 25% aqueous glutaraldehyde (Sigma Chemical, St. Louis, MO) was added to 0.9 mL of 10 or 20% (g protein/100 g water) solutions of BSA in deionized H_2O contained in 5 or 10 mm tubes; gels formed within 10 min. The gels in D_2O were prepared by adding 0.1 mL of 25% aqueous glutaraldehyde to 0.9 mL of 15% BSA solution in D_2O. The gel was soaked in D_2O for 48 h with three changes of D_2O per day then placed in a 10-mm tube for measurement. The hydrated protein samples were prepared to contain 0.32 g water per 1.0 g of protein by adding water to the lyophilized protein and equilibrating for at least 3 days at 310 K. The water content was measured using a Karl Fischer titrator (Aquatest 8; Photovolt Instruments, Indianapolis, IN).

The nuclear spin relaxation rates at Larmor frequencies between 0.01–30 MHz were recorded using a Stelar FFC-2000 spectrometer (Stelar, Mede, Italy). The field-switching time was 3 ms, the polarization field was 30 MHz and free induction decays were recorded after a single (5.5 μs) 90° excitation pulse applied at 15.8 MHz using a receiver-delay time of 11 μs. Temperature was controlled using a Stelar VTC90 variable temperature controller, which was calibrated using an external thermocouple inserted into a surrogate sample at the resonance position in the probe.

The NMR experiments for proton Larmor frequencies between 36–300 MHz were made using the fringe field of a 7.05 T magnet (Magnex Scientific, Oxford, UK) operating in conjunction with a Tecmag Apollo transceiver (Tecmag, Houston, TX), Miteq preamplifier (Miteq, Haupaug, NY), an AMT power amplifier (American Microwave Technologies, Brea, CA) and a probe constructed in this laboratory using a transmission-line design. The 90° pulse length was 8.5 μs. The sample was polarized in the resonance field of the superconducting magnet, after which the magnetization was inverted with a 180° pulse. The sample, then, was pneumatically shuttled to a calibrated position in the fringe field of the 7.05 T magnet for a variable relaxation delay and pneumatically returned to the resonance field, where the spectrum was promptly recorded using a 90° pulse. The integrated intensity of the NMR signal measured as a function of the relaxation delay provided the relaxation rate at the value of the calibrated fringe-field position. Within experimental error, all the decay/recovery curves of longitudinal magnetization were exponential. Fringe-field measurements were conducted at ambient laboratory temperature of ~20°C.

RESULTS

Fig. 1 shows the protein-proton magnetic relaxation dispersion profile for dry BSA and a cross-linked gel at 15 g BSA/100 g of D_2O. The water is strongly depleted in ^1H and labile protein protons have been exchanged for deuterons by successive exchanges from D_2O to minimize mobile ^1H. The data sets are identical within experimental error except that deuteration of the amide protons decreases the effects of proton coupling to the amide ^{14}N at magnetic field when the proton transitions match or cross the ^{14}N transitions in the 0.5–3 MHz range (24,25). The deuteration adds similar cross-relaxation peaks between the immobilized deuterons and the protons around 0.1–0.2 MHz. The environment in the cross-linked gel is highly aqueous and the protein structure is native. The protein is made rotationally immobile by the cross-linking reaction, and yet the magnetic relaxation dispersion (MRD) profile reproduces that for the dry solid. Therefore, by the measure of the magnetic-field dependence of the protein-proton-spin-lattice-relaxation-rate constant, the hydration effects on the protein-proton-spin-lattice-relaxation-dispersion profile are negligible if the water is ^2H_2O. The variety of water-protein interactions associated with the full hydration of the protein does not alter the underlying

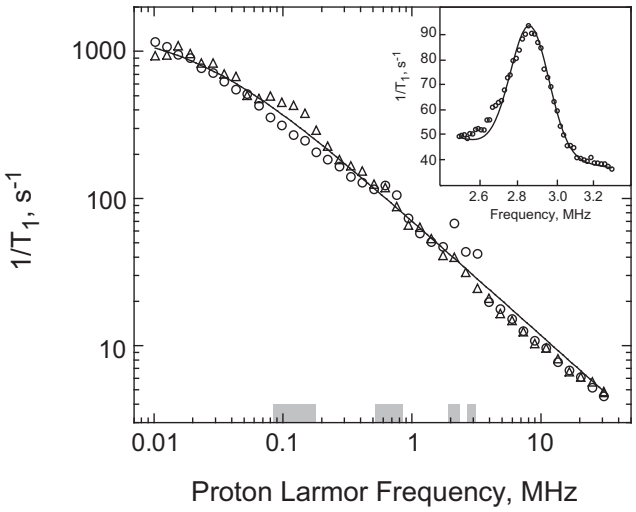

FIGURE 1 Proton spin-lattice relaxation rate constants as a function of the magnetic field strength plotted as the proton Larmor frequency for dry BSA (*open circles*) and deuterated 15% BSA gel in D_2O (*triangles*) at 302 K. The solid line is the best fit to the first term of Eq. 1 with $b = 0.782$. The second moment, $M_2 = 7.98 \times 10^9$ s^{-2}, was measured from the free induction decay and the dipolar coupling strength was calculated as $\omega_{dip} = \sqrt{20M_2/9}$. The peaks in the relaxation profiles are due to ^{14}N-^1H and ^2H-^1H heteronuclear relaxation pathways that become efficient when transition energies at the positions of the gray blocks on the frequency axis. The inset shows one of the ^{14}N-^1H peaks for dry BSA; it has Gaussian shape centered at 2.86 ± 0.01 MHz and the full width at the half height of 256 ± 20 kHz.

protein dynamics that cause the fluctuations in the proton-proton-dipole-dipole couplings that drive the spin-relaxation process. This observation does not depend on the details of the model for the nuclear spin-lattice-relaxation process and is somewhat different from our earlier conclusion based on MRD studies of proteins as a function of water content over a limited range of magnetic field strengths as discussed below.

Neglecting the ^{14}N and ^2H quadrupole relaxation peaks, the theory for the dry protein is summarized in Eq. 1 (3):

$$\frac{1}{T_1} = 4\pi k_B T M_2 h d_s \left\{ \frac{3}{4}\frac{1}{E_{v\|}^2}\left(1+\frac{1}{2^b}\right)\left(\frac{h\omega_o}{E_{v\|}}\right)^{-b} + \frac{1}{6}\frac{1}{E_{v\perp}^2}\left(\frac{7}{2}+\frac{1}{2^b}\right)\left(\frac{h\omega_o}{E_{v\perp}}\right)^{-b}\right\}, \quad (1)$$

where M_2 is the proton second moment, d_s the spectral dimension, $E_{v\|}$ and $E_{v\perp}$ are the vibrational frequencies for parallel and perpendicular motions of the polypeptide chain, ω_o is the nuclear Larmor frequency, $b = 3 - 2d_s/d_f - d_s$, and the other symbols have their usual meaning. The vibrational frequencies present a challenge; we have used the amide (*I*) frequency for the parallel mode of 1560 cm^{-1}. The perpendicular mode appropriate to the whole chain is somewhat smaller; originally we assumed a value of order 200 cm^{-1} (3), but the more extensive data suggests that this value is too small. As the two vibrational frequencies

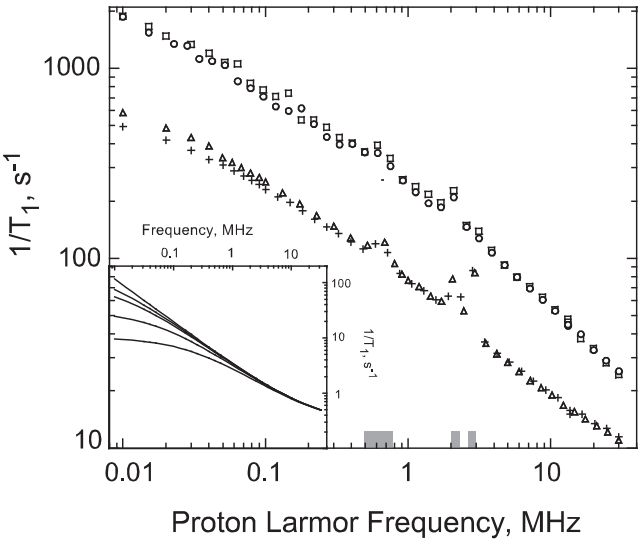

FIGURE 2 Protein-proton (○) and water-proton (□) relaxation rate constants as a function of proton Larmor frequency for BSA hydrated to the level of 0.32 g water/g protein at −40°C and protein-proton (△) and water-proton (+) relaxation rate constants at 28°C for the same sample. The gray blocks along the frequency axis identify the ^{14}N transitions. The inset shows the slow relaxation constant as a function of Larmor frequency computed assuming that the protein protons relax with a power law with slope 0.78 and $F = 0.069$ appropriate for 10% BSA gel for different values of the transfer rate constant from protein to water spins: from top to bottom 10^5, 200, 100, 50, 10, with the water rate constant set to 0.33 s^{-1}.

become similar, the importance of separating the terms for parallel and perpendicular contributions is lost. The solid line in Fig. 1 was obtained with just the first term of Eq. 1 using the Levenburg-Marquardt algorithm and the fit parameters are listed in the Fig. 1 legend.

Fig. 2 summarizes relaxation rates for water and protein protons in rehydrated lyophilized BSA samples. The water signal is isolated from the protein signal by sampling the free induction decay after the solid component has decayed. Extrapolation of this component to zero time permits isolation of the solid component or protein proton relaxation rate constant. In general, the magnetic coupling of the two spin populations produces two decay components for the longitudinal magnetization. Because of finite magnetic field switching times, we are experimentally restricted to observe the slowly decaying longitudinal component of the total proton magnetization whether we observe water or protein protons. This slow longitudinal magnetization decay constant is

$$\frac{1}{T_{1s}} = \frac{1}{2}\left\{\frac{1}{T_{1W}} + \frac{1}{T_{1P}} + \frac{1}{T_{WP}}\left(1 + \frac{1}{F}\right) - \left[\left(\frac{1}{T_{1P}} - \frac{1}{T_{1W}} - \frac{1}{T_{WP}}\left(1 - \frac{1}{F}\right)\right)^2 + \frac{4}{FT_{WP}^2}\right]^{\frac{1}{2}}\right\}, \quad (2)$$

where F the ratio of the number of solid protons to the number of water protons, $1/T_{1P}$ is the protein-proton-relaxation rate given by Eq. 1, $1/T_{WP}$ is the pseudo first order rate constant for magnetization transfer between protein and water-proton populations, and $1/T_{1W}$ is the bulk water-relaxation rate constant (8,26). At all magnetic field strengths, the observable relaxation constants scale with the relative size of the two proton populations (27).

At low temperature and low water content, the protein and water proton data are identical within experimental error and both spin populations report the same magnetic field dependence for the spin-lattice relaxation rate constant as shown in Fig. 2. At higher temperature or water contents, the water-proton profile falls below the protein proton profile at low frequency caused in part by data sampling errors for the protein spins, and because the magnetization transfer rate constant between the protein and water spins is concentration dependent. The Fig. 2 inset summarizes calculations of the MRD profile based on the assumption that the protein protons are described by a power law with an exponent of 0.78, the water proton relax with a field independent rate constant of 0.33, which neglects surface effects that are important at higher field strengths, and a protein-proton/water-proton ratio of 0.069 that is appropriate to a 10% BSA gel sample. The different profiles correspond to decreasing protein-to-water-proton-transfer-rate constants ranging from 10^5, which is in the strong coupling limit appropriate to a rigid solid, to 10, which clearly limits the low field relaxation rate constant to the magnetization transfer rate constant.

Fig. 3 summarizes relaxation dispersion profiles for a series of cross-linked BSA gels of different water content that correspond to values of F from 0.416 to 0.047. We observe the water protons because the signal is very large compared to the protein proton signal. The inset shows that the relaxation constant is a linear function of the quantity $F/1 + F$, which is the fraction of protons in the sample that belong to the solid pool. We note that this concentration dependence is not unique to this model. In particular, because the number of water-molecule-protein interactions is proportional to the protein concentration, a similar dependence is expected for relaxation in the absence of strong magnetic coupling between the water and protein protons.

The expanded relaxation-rate axis of Fig. 4 emphasizes the details of proton magnetic relaxation profiles of BSA gels in H_2O, the inset in Fig. 4 compares the relaxation dispersion profiles for dry BSA and 10% BSA gel in H_2O at 302 K, illustrating the differences between two dispersions on the same scale. Hydration of the protein with H_2O changes the MRD in several ways:

1. For the protein gel, the large pool of water protons is magnetically coupled to the pool of protein protons, which changes the observable relaxation-rate constants of both the protein and water protons. The effects of this magnetic coupling have been examined thoroughly and the consequences as a function of the magnetization transfer rate shown in Fig. 2 (8,26,27).

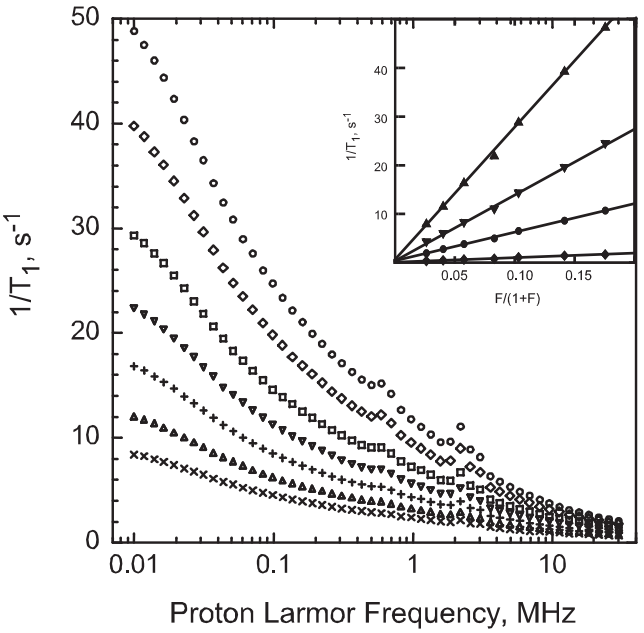

FIGURE 3 Water-proton relaxation-dispersion profile for bovine serum albumin cross-linked gels at different protein concentrations at 302 K: 40% (g protein/100 g water) (○), 30% (◇), 20% (□), 15% (▼), 10% (+), 7% (▲), and 4.5% (x). (*Inset*) The water-proton relaxation rate constant as a function of the protein proton fraction, $F/(1 + F)$, where F is the population ratio of protein to water protons at 30 MHz (◆), 1 MHz (●), 0.1 MHz (▼), and 0.01 MHz (▲).

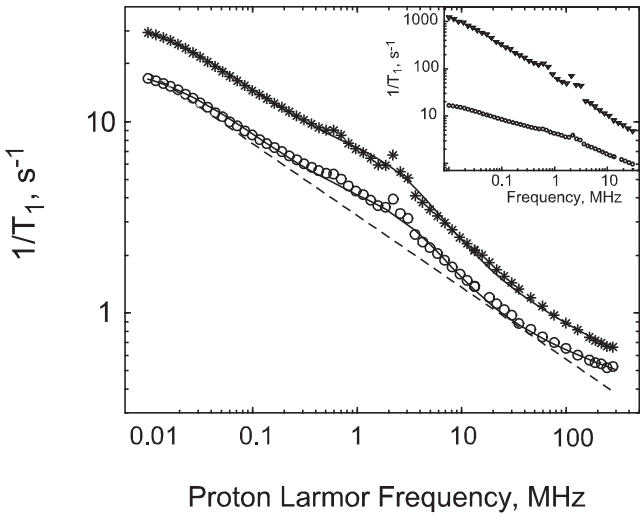

FIGURE 4 Water-proton $1/T_1$ as a function of the magnetic field strength plotted as the proton Larmor frequency for 10% (○) and 20% (*) bovine serum albumin gels at 298 K. Solid lines are the best fits to Eq. 2, where the protein-proton-relaxation rate is given by the Eq. 1 and the water proton relaxation rate by Eq. 3. The second moment, $M_2 = 4.56 \times 10^9\ s^{-2}$, was measured from the free induction decay (54). $1/T_1^0$ was fixed at 0.33 and $1/T_1^{sur}$ was calculated as described in Grebenkov et al. (39) with a correlation time of 15 ps. The bound water contribution, $1/T_1^{bnd}$, is given by Eq. 4. The best-fit parameters for the power law exponent and correlation time for bound water stochastic jumps are 0.75 and 41 ns respectively for the 10% gel and 0.74 and 49 ns for the 20% gel. Additional parameters include the magnetization transfer rate, $1/T_{1,WP}$, factor $C\frac{N_L}{N_H}$ (Eq. 4), and a scaling factor associated with the strength of the dipolar coupling for water translational surface diffusion (37). The 5-parameter fit to these data is not unique; however, the values of these last parameters do not affect the value deduced for the motion of protein-bound water molecules. The dashed straight line is for reference. The inset compares the relaxation rate-constants of Fig. 1 with those of the H_2O-hydrated systems in Fig. 4.

2. The low-field-relaxation rates in H_2O deviate from the power law, which is caused in part by the effects of finite magnetization transfer between the protein protons and the water protons as shown in Fig. 2. We note that at sufficiently low magnetic field strengths a second cause for a plateau in the field dependence is that for the solid-spin system, the effective magnetic field cannot drop below the local magnetic field created by the neighboring magnetic dipoles in the solid, i.e., the local dipolar field (28); however, other experiments suggest that it is of minor importance in these cases.
3. The shape of the magnetic field dependence in Fig. 4 is changed from that in Fig. 1. The ^1H relaxation rates in H_2O samples are larger than in D_2O samples at Larmor frequencies >5 MHz. When ^1H_2O relaxation-rate constants were measured only to a proton Larmor frequency of 30 MHz, the high field region appeared to be a plateau deriving from a different class of motions such as surface dynamics of water. However, several different NMR relaxation approaches using ^1H, ^2H, and ^{17}O show that the relaxation caused by motions of water at the protein surface are relatively unimportant in this frequency range because they are orders of magnitude faster than the reciprocal of these Larmor frequencies (27,29). This conclusion is consistent with earlier NMR measurements using paramagnetic localization of diffusive contributions to relaxation (30), high resolution NMR measurements (31), neutron diffraction measurements (32), optical spectroscopy (33), and molecular dynamics simulations (34,35). When the proton-relaxation rates are measured to sufficiently high magnetic field strengths, the relaxation rates at high field return to an extrapolation of the low-field MRD profile and in the intermediate range of fields there is an additional contribution or a ''bump'' in the field dependence. This intermediate field bump is absent when the protein is hydrated with D_2O even to the level of a gel as shown in Fig. 1. One might suspect that hydration could significantly affect side-chain motions and that the bump derives from such a dynamical consequence of hydration. However, this source would be fully active in the samples hydrated with D_2O, which is not observed. Therefore, this effect is caused by the water protons.

Substitution of ^2H for ^1H exchanges deuterons for protons at labile nitrogen and oxygen positions on the protein. The dipolar coupling between the amide ^1H at and ^{14}N, which relaxes rapidly by a nuclear electric quadrupole mechanism, causes the peaks in the relaxation-rate profile when the

nitrogen and proton frequencies match. These peaks occur close to the pure nuclear quadrupole resonance frequencies of the nitrogen, i.e., at ~0.8, 2.4, and 2.8 MHz. One may suppose that the protonation of the nitrogen sites and the consequent additional relaxation pathway through the nitrogen spin system could cause the relaxation bump of Fig. 4. However, as shown by the inset of Fig. 1, these quadrupole features are much narrower than that of the broad relaxation contribution in Fig. 4. Therefore, we conclude that dynamics associated with the water molecule protons causes the broad relaxation contribution in the H_2O hydrated protein cases.

DISCUSSION

The magnetic field dependence of the protein-proton $1/T_1$ in Fig. 1 is described by the same power-law exponent for the hydrated protein gel as the lyophilized solid provided that the water protons are replaced by deuterons, which are not magnetically well coupled to the protein protons. This lack of spin coupling occurs because the magnetogyric ratio of the deuteron is smaller than that for the proton by approximately a factor of 6 that enters the relaxation equation as the square (36). Therefore, cross-relaxation between protons and deuterons is weak.

If we adopt the spin-fracton model for $1/T_{1\mathrm{p}}$, the power law exponent, b, has been related to d_f, the fractal distribution of mass in the protein, and d_s, the spectral dimension characterizing the distribution of vibrational states and the propagation of the structural disturbances that create relaxation (3). Values of d_f in proteins have been reported for a large number of proteins to range from 2.3–3.0 and depend somewhat on how d_f is computed (17,18). That the value of b is 0.78 regardless of the hydration in D_2O implies a constraint on the spectral dimension, d_s. It is shown elsewhere (3) that $b = 3 - 2d_\mathrm{s}/d_\mathrm{f} - d_\mathrm{s}$; setting $b = 0.78$ and $2.3 < d_\mathrm{f} < 3.0$ implies that the value of d_s is constrained between 1.19 and 1.33. We note that for the gel shown in Fig. 1, the proteins are covalently connected by cross-link bridges that create an interconnected molecular network that fills the sample volume. Computational approaches based on network models for the protein dynamics have suggested that the value of d_s depends on molecular mass (16,37). In these experiments this may imply that the value of b should depend on molecular size; however, within experimental error we see no difference between the uncross-linked dry protein and the cross-linked network. Of course, it is possible that there may be changes in d_f on hydration that compensate for changes in d_s and maintain the value of b constant. These data do not test this possibility. In addition, the lyophilized condition provides intermolecular contacts that may alter the effective connectivity in the spirit of network models, but the dynamic consequences of these intermolecular contact interactions are unclear. It may seem surprising that the exponent b is not sensitive to the addition of solvent in light of recent discussions of solvent slaving or protein dynamics (38); however, the spin relaxation is dominated by small scale displacements that modulate the dipolar coupling and is insensitive to rare large scale fluctuations. Therefore, these observations do not address the validity of the solvent slaving ideas.

Fig. 2 shows that at low water content and temperature, the strong magnetic coupling limit is satisfied and that the water protons and the protein protons report identical relaxation dispersion profiles. The rate constant, $1/T_\mathrm{wp}$, is a pseudo first-order-rate constant describing an intermolecular cross-relaxation process. Therefore, $1/T_\mathrm{wp}$ is implicitly a function of the size the participating proton pools because of detailed balance. As the water population grows relative to the protein population, the effective transfer rate constant drops, and the consequence is that the cross-relaxation contribution to the proton relaxation profile develops a low-field plateau as shown in Fig. 2. The calculations shown in the Fig. 2 inset range from the very strong coupling limit where the power law of the protein spin system is transferred to the water protons at all field strengths, to transfer rate limited case with a transfer rate of 10; nevertheless, when the protein-proton-relaxation-rate constants drop with increasing field, the higher field portions of the profile satisfy the strong coupling constraints. Therefore, the importance of the water-protein-proton-cross-relaxation rate is both magnetic field and composition dependent. The cross-relaxation contributions are significant at all frequencies even when limited by the effective magnetization transfer rate constant. At Larmor frequencies >10 MHz, the intermolecular cross-relaxation effects will usually be in the strong coupling limit.

Fig. 3 summarizes relaxation dispersion data for a series of BSA gels that span a significant range of the composition variable F. The increase in relaxation rate with concentration at all Larmor frequencies is consistent with Eq. 2. However, as noted, this dependence does not distinguish between models that depend on the effective concentration of bound labile water molecules or protons.

In the strong magnetic coupling limit, the total observable water-proton- spin-lattice-relaxation-rate constant is generally a function of the rate constants for the protein protons, the water protons, and the cross-relaxation between these two populations as summarized in Eq. 2. In earlier discussions, the water relaxation-rate constant in hydrated protein systems was treated as independent of frequency because there was no evidence that there were water correlation times that were as slow as the Larmor frequencies studied except for the chemical exchange processes that contribute to the cross-relaxation rate. The magnetic field dependence of the observed ^1H_2O relaxation rate was ascribed to the protein-proton population (3), which is a power law as shown in Fig. 1. Comparison of Fig. 1 and Fig. 4 shows that there are field dependent water-proton contributions. For the relaxation of water protons we may write

$$\frac{1}{T_1^{w}(\omega)} = \frac{1}{T_1^{o}} + \sum_i \frac{1}{T_{1i}^{bnd}(\omega)} + \sum_j \frac{1}{T_{1j}^{sur}(\omega)}, \qquad (3)$$

where $T_1{}^{o}$ is the relaxation time for bulk water and is field independent in the frequency range of present magnetic field strengths, $T_{1i}{}^{bnd}$ is the relaxation time for water bound to the protein in the ith site, and $T_{1j}{}^{sur}$ is the relaxation time for the water molecule at the jth surface site and the sums include all sites. The surface site relaxation contributions are discussed in detail elsewhere but make contributions that are logarithmic in the Larmor frequency and important only at the highest field strengths (39).

There are two classes of motion for bound water molecules in a protein binding site: 1), in a site without hydrogen bonds between the water and a protein donor or acceptor, the entrapped water may reorient by stochastic rotational diffusion within the angles permitted by the confinement; and 2), in a site where the water may be constrained by hydrogen bonds to the protein, it may reorient stochastically as the bonding pattern permits but the motions of the water and the surrounding protein are dynamically coupled by the intermolecular connection. These two classes of motion produce qualitatively different dependence of the spin-lattice-relaxation-rate constant on the magnetic field strength. For the uncoupled case, the relaxation may be modeled as a Lorentzian contribution; the effect is that the high field portion of the MRD profile returns to an extrapolation of the low field relaxation profile. In the dynamically coupled case, where water molecules couple to the protein for time longer then characteristic correlation time of protein backbone fluctuations, the relaxation equation is not a simple Lorentzian and the high-field relaxation rates are displaced to higher values compared to an extrapolation of the low field rates (13,40). Either approach provides an acceptable fit to the data with a correlation time between 20–50 ns. The solid lines in Fig. 4 result from fits to Eq. 2, using the tethered local dynamic model for bound water contribution. Although there may be a distribution of effective local correlation times for the long-lived-water sites in the protein, no distribution function is necessary with either model to provide an adequate description of the data. It is, of course, possible that both classes of motion contribute.

A correlation time of 20–50 ns is within a factor of 2 of the global rotational correlation time for the protein in solution. This near degeneracy of the local motion with the global reorientation correlation time will make this motion difficult to observe in solution phase MRD experiments (41). The low-frequency amplitude of the MRD profile for a protein solution is proportional to the number of long-lived or bound water molecules (42). For serum albumin, we and others have reported 25 $\pm$ 3 such water molecules if it is assumed that there is no local motion of the water in the bound sites; i.e., that all internal water is rigid and reorients with the global rotational correlation time of the protein (29,43,44). In fact, $N \times S^2$ is measured where S is a generalized order parameter, N is the number of bound water molecules, and this product for serum albumin is 25. The local motion detected in this work as an important contribution to the total proton relaxation of the nonrotating protein spin system implies that at least some water molecules suffer a local motion with an average correlation time of 20–50 ns. Therefore, S^2 may be <1, but the near degeneracy of the local and global reorientation implies that the separation of local and global dynamics may be problematic for at least some bound water molecules (41) and quantitative refinement of the number of bound water molecules based on the amplitude of the solution phase relaxation dispersion profile remains a challenge. Some have advanced the idea that the bound water molecules cannot move sufficiently to affect relaxation significantly (45). It is unclear that the protein is sufficiently rigid for this possibility to account for all bound water molecules. Even the polypeptide backbone retains sufficient motion for the ^{14}N to provide a relaxation sink for the proton-spin population even when global rotation is stopped as shown in Fig. 1.

If the strong coupling approximation fails in the frequency range of the bump, the critical importance of the water-proton contribution remains. If one rejects local motions of bound water molecules as the cause of the bump, then a Lorentzian contribution to ^1H relaxation may be obtained by a water-molecule-exchange process that modulates both the inter and intramolecular dipolar couplings as advanced by Halle and co-workers in the EMOR model (19,20). Because it is difficult to dismiss relaxation coupling at all frequencies studied here, and the chemical exchange that interrupts the dipolar couplings is critical to carry the magnetization transfer between the protein and the water spins, it is reasonable in this case to presume that both an exchange process as described by the EMOR model and cross-relaxation contribute to the total relaxation. As before, the deviations from the power law shown in Fig. 4 require only a single Lorentzian where now the correlation time is interpreted as a water-molecule-exchange time. Although the character of the motions presumed in each approach is different, the correlation time deduced is the same.

The water-molecule motions with correlation times in the tens of ns range correspond to frequencies of order 10^7 s^{-1} and these motions affect the dielectric properties of the environment. To the extent that one may use continuum concepts in a localized context, the dielectric response in the vicinity of the dynamically inhibited water molecules must be frequency dependent with a dispersion associated with the characteristic dynamics similar to that observed magnetically here. Correspondingly, one expects the electrostatic contribution to the energetic cost of conformational changes is influenced by the perturbed local dielectric constant. In the context of transition-state theory, the free energy barrier for structural rearrangement may be tuned by the number and dynamical characteristics of semimobile water molecules in the critical regions of the protein structure (46,47).

These results support conclusions drawn from dielectric dispersion measurements on hydrated proteins (48–51).

The magnitude of the bound water contribution to the MRD profile for rotationally immobilized protein in the intermediate field range of tens of MHz for the proton Larmor frequency is significant and partly masks the power-law that derives from the protein structural fluctuations. The combination of this contribution and the low-field limitations in the magnetization-transfer-rate constant alters the magnetic field dependence. Data over a limited field range, 0.01 to tens of MHz may be fitted by a power law with a smaller exponent. It is now clear that with more complete measurement of the magnetic field dependence of the relaxation-rate constants, the underlying power-law parameters are practically the same as in the dry protein or protein hydrated with ^2H_2O as in Fig. 1. Thus, the apparent water-content dependence of the power-law exponent is not supported by the more extensive data now available over the wider range of magnetic fields. Structural changes attending hydration do not affect the power-law exponent significantly, although spectral changes are clearly detected in magic-angle spinning NMR measurements on crystalline and noncrystalline proteins (52,53).

The power law in the Larmor frequency describes the ^1H relaxation-dispersion profile over the nearly 5 decades in frequency shown in Fig. 1. Further, the same power law is maintained as the protein is hydrated with ^2H_2O that is known to facilitate side-chain motion at the surface (13,54). Therefore, these side-chain motions are not critical in the underlying relaxation process in this range of frequencies. The anomalous dispersion relation included in the spin-fracton theory relates the frequency ω to a length scale l according to the anomalous dispersion law (3,6); $\omega \propto l^{-df/ds}$ where d_s is the spectral dimension characterizing the propagation of fluctuations in the structure. Therefore, the frequency axes in Fig. 1 and Fig. 4 may also correspond to a length axis, the larger the frequency the smaller the length scale. The persistence of the power law from 10 kHz to 300 MHz implies that the character of the fluctuation is scale invariant over the nearly 4 or 5 decades shown in Fig. 4, which is consistent with a system described by fractal characteristics in both the spatial and spectral properties. The imperfect connectivity in the protein causes confinement of fluctuations and a dramatic increase in the density of low frequency modes relative to a classical 3D network. This conclusion is supported by network model calculations as noted earlier (16). As discussed previously (6), the relaxation-rate constant, $1/T_1$, is proportional to the frequency dependence of the mean-square displacement that varies as a power law ω^{ds-2}. With the MRD experiment, we interrogate frequencies that are lower than those sampled by most other methods. Nevertheless, these measurements demonstrate that the displacement amplitudes increase according to the same power law over the frequency range that extends well into that for catalytic rate constants. As noted by Doruker et al. (55), the contributions of the low frequency modes make the largest contributions to the mean-square displacements. Although based on different theoretical development, these results imply constraints on the value of d_s that are similar to predictions based on Gaussian network models for the protein (16).

CONCLUSIONS

Rotational immobilization of the protein provides the opportunity to examine the dynamics of both the protein and associated water in time regimes that are not directly accessible for proteins in solution because of rotational averaging of dipolar couplings by global rotation of the protein. The ^1H magnetic relaxation dispersion profile over the Larmor frequency range from 0.01 to 300 MHz for rotationally immobilized proteins is described by a power law in the Larmor frequency that is independent of the hydration level of the protein provided that water ^1H is replaced by ^2H. Therefore, the character of the underlying protein dynamics that determine the nature of the fluctuations in the proton-proton dipolar couplings, which drive spin relaxation, is not substantially altered over this frequency range and is consistent with a spin-fracton relaxation theory where the values of the spectral dimension and fractal dimension for the distribution of mass are either constant or change in compensating ways as a function of hydration. In contrast, hydration with H_2O provides an additional ^1H-relaxation mechanism caused by motions of rare bound water molecules in the range of 20–50 ns at 302 K. By comparison, water motions at the protein surface are characterized by correlation times in the range of tens of picoseconds and make only small contributions to the total observed spin relaxation in cross-linked protein systems or hydrated solids over this range of Larmor frequencies.

Helpful discussions with P. Levitz, J. Klafter, D. Petit, and B. Sapoval are gratefully acknowledged.

This work was supported by the National Institutes of Health (RO1 NIBIB2805), the University of Virginia, and the CNRS, France.

REFERENCES

1. Bryant, R. G., D. A. Mendelson, and C. C. Lester. 1991. The magnetic field dependence of proton spin relaxation in tissues. *Magn. Reson. Med.* 21:117–126.
2. Koenig, S. H., and R. D. Brown, 3rd. 1985. The importance of the motion of water for magnetic resonance imaging. *Invest. Radiol.* 20:297–305.
3. Korb, J.-P., and R. G. Bryant. 2001. The physical basis for the magnetic field dependence of proton spin-lattice relaxation rates in proteins. *J. Chem. Phys.* 115:10964–10974.
4. Nusser, W., and R. Kimmich. 1990. Protein backbone fluctuations and NMR field-cycling relaxation spectroscopy. *J. Phys. Chem.* 94: 5637–5639.
5. Korb, J.-P., and R. G. Bryant. 2004. Magnetic field dependence of proton spin-lattice relaxation of confined proteins. *C.R. Phys.* 5: 349–357.
6. Korb, J.-P., and R. G. Bryant. 2005. Noise and functional protein dynamics. *Biophys. J.* 89:2685–2692.
7. Korb, J.-P., and R. G. Bryant. 2002. Magnetic field dependence of proton spin-lattice relaxation times. *Magn. Reson. Med.* 48:21–26.

8. Lester, C. C., and R. G. Bryant. 1991. Water-proton nuclear magnetic relaxation in heterogeneous systems: hydrated lysozyme results. *Magn. Reson. Med.* 22:143–153.
9. Grad, J., and R. G. Bryant. 1990. Nuclear magnetic cross-relaxation spectroscopy. *J. Magn. Reson.* 90:1–8.
10. Goldman, M. 1970. Spin Temperature and Nuclear Magnetic Resonance in Solids. Oxford University Press, London.
11. Kimmich, R., N. Fatkullin, …, K. Gille. 1998. Chain dynamics in entangled polymers: power laws of the proton and deuteron spin-lattice relaxation dispersions. *J. Chem. Phys.* 108:2173–2177.
12. Korb, J.-P., A. Van-Quynh, and R. Bryant. 2001. Low-frequency localized spin-dynamical coupling in proteins. *Comptes Rendus de l'Academie des Sciences Series IIC Chemistry*. 4:833–837.
13. Goddard, Y., J.-P. Korb, and R. G. Bryant. 2007. The magnetic field and temperature dependences of proton spin-lattice relaxation in proteins. *J. Chem. Phys.* 126:175105.
14. Orbach, R. 1986. Dynamics of fractal networks. *Science*. 231:814–819.
15. Granek, R., and J. Klafter. 2005. Fractons in proteins: can they lead to anomalously decaying time autocorrelations? *Phys. Rev. Lett.* 95:098106.
16. Reuveni, S., R. Granek, and J. Klafter. 2008. Proteins: coexistence of stability and flexibility. *Phys. Rev. Lett.* 100:208101.
17. Enright, M. B., and D. M. Leitner. 2005. Mass fractal dimension and the compactness of proteins. *Phys. Rev. E.* 71:01191.
18. Enright, M. B., X. Yu, and D. M. Leitner. 2006. Hydration dependence of the mass fractal dimension and anomalous diffusion of vibrational energy in proteins. *Phys. Rev. E.* 73:051905.
19. Chávez, F. V., and B. Halle. 2006. Molecular basis of water proton relaxation in gels and tissue. *Magn. Reson. Med.* 56:73–81.
20. Halle, B. 2006. Molecular theory of field-dependent proton spin-lattice relaxation in tissue. *Magn. Reson. Med.* 56:60–72.
21. Persson, E., and B. Halle. 2008. Cell water dynamics on multiple time scales. *Proc. Natl. Acad. Sci. USA.* 105:6266–6271.
22. Martin, R. W., and K. W. Zilm. 2003. Preparation of protein nanocrystals and their characterization by solid state NMR. *J. Magn. Reson.* 165:162–174.
23. Morcombe, C. R., V. Gaponenko, …, K. W. Zilm. 2005. ^{13}C CPMAS spectroscopy of deuterated proteins: CP dynamics, line shapes, and T_1 relaxation. *J. Am. Chem. Soc.* 127:397–404.
24. Kimmich, R., W. Nusser, and F. Winter. 1984. In vivo NMR field-cycling relaxation spectroscopy reveals $^{14}N^1H$ relaxation sinks in the backbones of proteins. *Phys. Med. Biol.* 29:593–596.
25. Winter, F., and R. Kimmich. 1985. $^{14}N^1H$ and $^2H^1H$ cross-relaxation in hydrated proteins. *Biophys. J.* 48:331–335.
26. Edzes, H. T., and E. T. Samulski. 1977. Cross relaxation and spin diffusion in the proton NMR or hydrated collagen. *Nature*. 265:521–523.
27. Bryant, R. G. 1996. The dynamics of water-protein interactions. *Annu. Rev. Biophys. Biomol. Struct.* 25:29–53.
28. Kimmich, R., G. Schnur, and A. Scheuermann. 1983. Spin-lattice relaxation and lineshape parameters in nuclear magnetic resonance of lamellar lipid systems: fluctuation spectroscopy of disordering mechanisms. *Chem. Phys. Lipids.* 32:271–322.
29. Denisov, V. P., and B. Halle. 1996. Protein hydration dynamics in aqueous solution. *Faraday Discuss.* 103:227–244.
30. Polnaszek, C. F., and R. G. Bryant. 1984. Nitroxide radical induced solvent proton relaxation: measurement of localized translational diffusion. *J. Chem. Phys.* 81:4038–4045.
31. Otting, G., E. Liepinsh, and K. Wüthrich. 1991. Protein hydration in aqueous solution. *Science*. 254:974–980.
32. Gabel, F., D. Bicout, …, G. Zaccai. 2002. Protein dynamics studied by neutron scattering. *Q. Rev. Biophys.* 35:327–367.
33. Pal, S. K., J. Peon, …, A. H. Zewail. 2002. Biological water: femtosecond dynamics of macromolecular hydration. *J. Phys. Chem. B.* 106:12376–12395.
34. Dastidar, S. G., and C. Mukhopadhyay. 2003. Structure, dynamics, and energetics of water at the surface of a small globular protein: a molecular dynamics simulation. *Phys. Rev. E.* 68:021921–021929.
35. Rocchi, C., A. R. Bizzarri, and S. Cannistraro. 1998. Water dynamical anomalies evidenced by molecular-dynamics simulations at the solvent-protein interface. *Phys. Rev. E.* 57:3315–3325.
36. Abragam, A. 1961. The Principles of Nuclear Magnetism. Oxford University Press, Oxford.
37. Burioni, R., D. Cassi, …, A. Vulpiani. 2004. Topological thermal instability and length of proteins. *Proteins*. 55:529–535.
38. Fenimore, P. W., H. Frauenfelder, …, F. G. Parak. 2002. Slaving: solvent fluctuations dominate protein dynamics and functions. *Proc. Natl. Acad. Sci. USA.* 99:16047–16051.
39. Grebenkov, D. S., Y. A. Goddard, …, R. G. Bryant. 2008. Dimensionality of water diffusive exploration at the protein interface in solution. *J. Phys. Chem. B.* 113:13347–13356.
40. Goddard, Y., J.-P. Korb, and R. G. Bryant. 2007. Nuclear magnetic relaxation dispersion study of the dynamics in solid homopolypeptides. *Biopolymers.* 86:148–154.
41. Lipari, G., and A. Szabo. 1982. Model-free approach to the interpretation of nuclear magnetic resonance relaxation in macromolecules. 1. Theory and range of validity. *J. Am. Chem. Soc.* 104:4546–4559.
42. Kiihne, S., and R. G. Bryant. 2000. Protein-bound water molecule counting by resolution of (1)H spin-lattice relaxation mechanisms. *Biophys. J.* 78:2163–2169.
43. Denisov, V. P., B. H. Jonsson, and B. Halle. 1999. Hydration of denatured and molten globule proteins. *Nat. Struct. Biol.* 6:253–260.
44. Denisov, V. P., J. Peters, …, B. Halle. 1996. Using buried water molecules to explore the energy landscape of proteins. *Nat. Struct. Biol.* 3:505–509.
45. Persson, E., and B. Halle. 2008. Nanosecond to microsecond protein dynamics probed by magnetic relaxation dispersion of buried water molecules. *J. Am. Chem. Soc.* 130:1774–1787.
46. Prakash, M. K., and R. A. Marcus. 2007. An interpretation of fluctuations in enzyme catalysis rate, spectral diffusion, and radiative component of lifetimes in terms of electric field fluctuations. *Proc. Natl. Acad. Sci. USA.* 104:15982–15987.
47. Prakash, M. K., and R. A. Marcus. 2008. Dielectric dispersion interpretation of single enzyme dynamic disorder, spectral diffusion, and radiative fluorescence lifetime. *J. Phys. Chem. B.* 112:399–404.
48. Jansson, H., R. Bergman, and J. Swenson. 2005. Relation between solvent and protein dynamics as studied by dielectric spectroscopy. *J. Phys. Chem. B.* 109:24134–24141.
49. Mijovic, M., Y. Bian, …, B. Chen. 2005. Dynamics of proteins in hydrated state and in solution as studied by dielectric relaxation spectroscopy. *Macromolecules.* 38:10812–10819.
50. Rizvi, T. Z., and M. A. Khan. 2007. Dielectric relaxation in singly hydrated bovine tendon collagen. *J. Phys. D. Appl. Phys.* 40:25–30.
51. Rizvi, T. Z., and M. A. Khan. 2008. Temperature dependent dielectric properties of slightly hydrated horn keratin. *Int. J. Biol. Macromol.* 42:292–297.
52. Morcombe, C. R., E. K. Paulson, …, K. W. Zilm. 2005. ^1H-^{15}N correlation spectroscopy of nanocrystalline proteins. *J. Biomol. NMR.* 31: 217–230.
53. Wylie, B. J., and C. M. Rienstra. 2008. Multidimensional solid state NMR of anisotropic interactions in peptides and proteins. *J. Chem. Phys.* 128:052207.
54. Diakova, G., Y. A. Goddard, …, R. G. Bryant. 2007. Changes in protein structure and dynamics as a function of hydration from (1)H second moments. *J. Magn. Reson.* 189:166–172.
55. Doruker, P., R. L. Jernigan, and I. Bahar. 2002. Dynamics of large proteins through hierarchical levels of coarse-grained structures. *J. Comput. Chem.* 23:119–127.